Structure and Properties of Neutron-Star Crusts with Brussels-Montreal Functionals

OUTER LAYER
1 meter thick
solid or liquid

CORE
10-15 kilometer deep
liquid

Nicolas Chamel

Institute of Astronomy and Astrophysics
Université Libre de Bruxelles, Belgium

in collaboration with:
J. M. Pearson, A. F. Fantina, S. Goriely, P. Haensel, J. L. Zdunik,
T. Delsate, N. Gürlebeck, Y. D. Mutafchieva, Zh. Stoyanov

CRUST
1 kilometer thick
solid

NEUTRON STAR

Hirschegg, 16 - 20 January 2017

Prelude
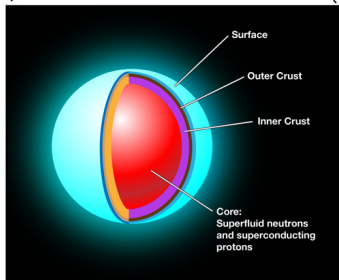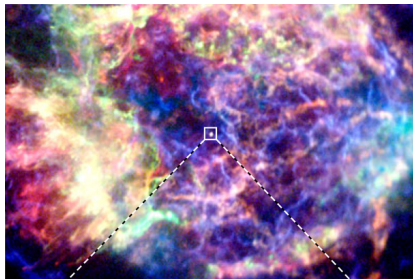
Although the crust of a neutron star represents about $\sim 1\%$ of the mass and $\sim 10\%$ of the radius, it is related to various phenomena:

- pulsar sudden spin-ups,
- X-ray (super)bursts,
- thermal relaxation in transiently accreting stars,
- quasiperiodic oscillations in soft gamma-ray repeaters
- r-process nucleosynthesis in neutron-star mergers
- mountains and gravitational wave emission

Plumbing neutron-star crusts
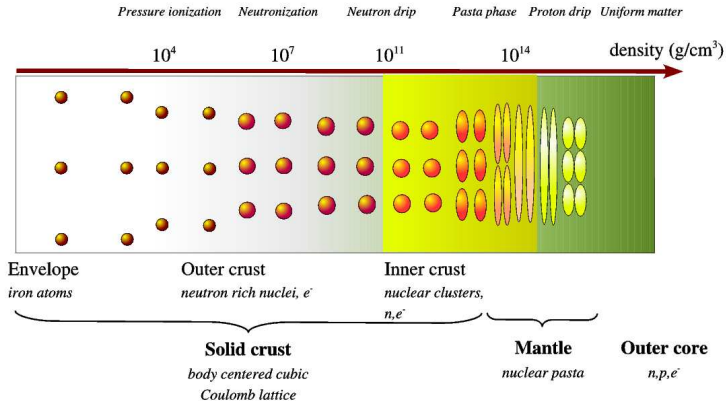
Chamel&Haensel, Living Reviews in Relativity 11 (2008), 10
http://relativity.livingreviews.org/Articles/lrr-2008-10/

The **nuclear energy density functional theory** provides a consistent and numerically tractable treatment of all these different phases.

Outline

Nuclear energy density functional theory in a nut shell

The energy E of a nuclear system ($q = n, p$ for neutrons, protons) is expressed as a (universal) functional of

- $n_q(\mathbf{r}, \sigma; \mathbf{r}', \sigma') = \; < \Psi | c_q(\mathbf{r}'\sigma')^\dagger c_q(\mathbf{r}\sigma) | \Psi >$
- $\widetilde{n}_q(\mathbf{r}, \sigma; \mathbf{r}', \sigma') = -\sigma' < \Psi | c_q(\mathbf{r}' - \sigma') c_q(\mathbf{r}\sigma) | \Psi >$,

where $c_q(\mathbf{r}\sigma)^\dagger$ and $c_q(\mathbf{r}\sigma)$ are the creation and destruction operators for nucleon q at position $\mathbf{r}$ with spin $\sigma = \pm 1$.

In turn, these matrices are expressed in terms of **independent quasiparticle** wavefunctions $\varphi_{1k}^{(q)}(\mathbf{r})$ and $\varphi_{2k}^{(q)}(\mathbf{r})$ as

$$n_q(\mathbf{r}, \sigma; \mathbf{r}', \sigma') = \sum_{k(q)} \varphi_{2k}^{(q)}(\mathbf{r}, \sigma) \varphi_{2k}^{(q)}(\mathbf{r}', \sigma')^*$$

$$\widetilde{n}_q(\mathbf{r}, \sigma; \mathbf{r}', \sigma') = -\sum_{k(q)} \varphi_{2k}^{(q)}(\mathbf{r}, \sigma) \varphi_{1k}^{(q)}(\mathbf{r}', \sigma')^* = -\sum_k \varphi_{1k}^{(q)}(\mathbf{r}, \sigma) \varphi_{2k}^{(q)}(\mathbf{r}', \sigma')^*.$$

The *exact* **ground-state energy** is obtained by minimizing the functional $E[n_q(\mathbf{r}, \sigma; \mathbf{r}', \sigma'), \widetilde{n}_q(\mathbf{r}, \sigma; \mathbf{r}', \sigma')]$ under the constraint of fixed nucleon numbers (and completeness relations on $\varphi_{1k}^{(q)}(\mathbf{r})$ and $\varphi_{2k}^{(q)}(\mathbf{r})$).

Hartree-Fock-Bogoliubov equations

Constrained variations of the nuclear energy functional yield the **self-consistent Hartree-Fock Bogoliubov** (HFB) equations

$$
\sum_{\sigma'} \int d^3 r' \begin{pmatrix} h_q(\mathbf{r}, \sigma; \mathbf{r'}, \sigma') & \widetilde{h}_q(\mathbf{r}, \sigma; \mathbf{r'}, \sigma') \\ \widetilde{h}_q(\mathbf{r}, \sigma; \mathbf{r'}, \sigma') & -h_q(\mathbf{r}, \sigma; \mathbf{r'}, \sigma') \end{pmatrix} \begin{pmatrix} \psi_{1k}^{(q)}(\mathbf{r'}, \sigma') \\ \psi_{2k}^{(q)}(\mathbf{r'}, \sigma') \end{pmatrix}
$$

$$
= \begin{pmatrix} E_k^{(q)} + \mu_q & 0 \\ 0 & E_k^{(q)} - \mu_q \end{pmatrix} \begin{pmatrix} \psi_{1k}^{(q)}(\mathbf{r}, \sigma) \\ \psi_{2k}^{(q)}(\mathbf{r}, \sigma) \end{pmatrix} ,
$$

where μ_q are the chemical potentials, and the non-local fields are defined by

$$
h_q(\mathbf{r}, \sigma; \mathbf{r'}, \sigma') = \frac{\delta E}{\delta n_q(\mathbf{r}, \sigma; \mathbf{r'}, \sigma')} , \qquad \widetilde{h}_q(\mathbf{r}, \sigma; \mathbf{r'}, \sigma') = \frac{\delta E}{\delta \widetilde{n}_q(\mathbf{r}, \sigma; \mathbf{r'}, \sigma')} .
$$

Duguet, Lecture Notes in Physics 879 (Springer-Verlag, 2014), p. 293

Dobaczewski & Nazarewicz, in "50 years of Nuclear BCS" (World Scientific Publishing, 2013), pp.40-60

Problem: we do not know what the exact functional is... We have thus to rely on phenomenological functionals.

Phenomenological nuclear energy density functionals

For simplicity, the functional is generally written as

$$E = \int \mathcal{E}\Big[n_q(\boldsymbol{r}), \boldsymbol{\nabla} n_q(\boldsymbol{r}), \tau_q(\boldsymbol{r}), \boldsymbol{J}_q(\boldsymbol{r}), \widetilde{n}_q(\boldsymbol{r}), \dots\Big] \, \mathrm{d}^3\boldsymbol{r}$$

where ($\boldsymbol{\sigma}_{\sigma\sigma'}$ denotes the Pauli spin matrices)

$$n_q(\boldsymbol{r}) = \sum_{\sigma=\pm 1} n_q(\boldsymbol{r}, \sigma; \boldsymbol{r}, \sigma), \quad \widetilde{n}_q(\boldsymbol{r}) = \sum_{\sigma=\pm 1} \widetilde{n}_q(\boldsymbol{r}, \sigma; \boldsymbol{r}, \sigma)$$

$$\tau_q(\boldsymbol{r}) = \sum_{\sigma=\pm 1} \int \mathrm{d}^3\boldsymbol{r}' \, \delta(\boldsymbol{r} - \boldsymbol{r}') \boldsymbol{\nabla} \cdot \boldsymbol{\nabla}' n_q(\boldsymbol{r}, \sigma; \boldsymbol{r}', \sigma)$$

$$\boldsymbol{J}_q(\boldsymbol{r}) = -\mathrm{i} \sum_{\sigma,\sigma'=\pm 1} \int \mathrm{d}^3\boldsymbol{r}' \, \delta(\boldsymbol{r} - \boldsymbol{r}') \boldsymbol{\nabla} n_q(\boldsymbol{r}, \sigma; \boldsymbol{r}', \sigma') \times \boldsymbol{\sigma}_{\sigma'\sigma}$$

Such functionals can be constructed from Skyrme type **zero-range effective interactions in the "mean-field" approximation**.

Remark: fitting directly the energy functional $\mathcal{E}$ to experimental and/or microscopic nuclear data may lead to self-interaction errors.
Chamel, Phys. Rev. C 82, 061307(R) (2010).

Phenomenological corrections for atomic nuclei

For atomic nuclei, we add the following corrections to the HFB energy:

- Wigner energy

$$E_W = V_W \exp\left\{ -\lambda\left(\frac{N-Z}{A}\right)^2 \right\} + V'_W|N-Z|\exp\left\{ -\left(\frac{A}{A_0}\right)^2 \right\}$$

$V_W \sim -2$ MeV, $V'_W \sim 1$ MeV, $\lambda \sim 300$ MeV, $A_0 \sim 20$

- rotational and vibrational spurious collective energy

$$E_{\text{coll}} = E_{\text{rot}}^{\text{crank}}\left\{ b\,\tanh(c|\beta_2|) + d|\beta_2|\,\exp\{-I(|\beta_2| - \beta_2^0)^2\} \right\}$$

This latter correction was shown to be in good agreement with calculations using 5D collective Hamiltonian.
Goriely, Chamel, Pearson, Phys.Rev.C82,035804(2010).

In this way, these collective effects do not contaminate the parameters (≤ 20) of the functional.

Brussels-Montreal Skyrme functionals (BSk)

Experimental data:

- all atomic masses with $Z, N \geq 8$ from the Atomic Mass Evaluation (root-mean square deviation: 0.5-0.6 MeV)
- nuclear charge radii
- symmetry energy $29 \leq J \leq 32$ MeV
- incompressibility $K_v = 240 \pm 10$ MeV (ISGMR)
  Colò et al., Phys.Rev.C70, 024307 (2004).

N-body calculations using realistic forces:

- equation of state of pure neutron matter
- $^1S_0$ pairing gaps in nuclear matter
- effective masses in nuclear matter
- stability against spin and spin-isospin fluctuations

Chamel et al., Acta Phys. Pol. B46, 349(2015)

Nonlocal and relativistic functionals have been also developed:
Goriely et al., Eur. Phys. J. A 52, 202 (2016).
Pena Arteaga, Goriely, Chamel, Eur. Phys. J. A 52, 320 (2016)

Brussels-Montreal Skyrme functionals

- ▷ **fit to realistic $^1S_0$ pairing gaps (no self-energy)** (BSk16-17)
  Chamel, Goriely, Pearson, Nucl.Phys.A812,72 (2008)
  Goriely, Chamel, Pearson, PRL102,152503 (2009).
  Chamel, Phys. Rev. C 82, 014313 (2010).

- ▷ **removal of spurious spin-isospin instabilities** (BSk18)
  Chamel, Goriely, Pearson, Phys.Rev.C80,065804(2009)
  Chamel & Goriely, Phys. Rev. C 82, 045804 (2010).

- ▷ **fit to realistic neutron-matter equations of state** (BSk19-21)
  Goriely, Chamel, Pearson, Phys.Rev.C82,035804(2010)

- ▷ **fit to different symmetry energies** (BSk22-26)
  Goriely, Chamel, Pearson, Phys.Rev.C88,024308(2013)

- ▷ **optimal fit of the 2012 AME** - rms 0.512 MeV (BSk27*)
  Goriely, Chamel, Pearson, Phys.Rev.C88,061302(R)(2013)

- ▷ **generalized spin-orbit coupling** (BSk28-29)
  Goriely, Nucl.Phys.A933,68(2015).

- ▷ **fit to realistic $^1S_0$ pairing gaps with self-energy** (BSk30-32)
  Goriely, Chamel, Pearson, Phys.Rev. C93,034337(2016).

Description of the outer crust of a neutron star

Main assumptions:

- matter is in full thermodynamic equilibrium
- the crust is stratified into pure layers made of nuclei $^A_Z X$
- atoms are fully pressure ionized $\rho \gg 10AZ$ g cm^{-3}
- electrons are uniformly distributed and are highly degenerate
- nuclei are arranged on a perfect body-centered cubic lattice
  $$T < T_m \approx 1.3 \times 10^5 Z^2 \left(\frac{\rho_6}{A}\right)^{1/3} \text{ K} \qquad \rho_6 \equiv \rho/10^6 \text{ g cm}^{-3}$$

The only microscopic inputs are nuclear masses. We have made use of the experimental data from the Atomic Mass Evaluation complemented with our HFB mass tables available at
http://www.astro.ulb.ac.be/bruslib/

Pearson,Goriely,Chamel,Phys.Rev.C83,065810(2011)

Electron polarization effects are included using the expressions given in *Chamel & Fantina,Phys.Rev.D93, 063001 (2016)*

Composition of the outer crust of a neutron star

The composition of the crust is completely determined by experimental nuclear masses down to about 200m for a 1.4$M_\odot$ neutron star with a 10 km radius
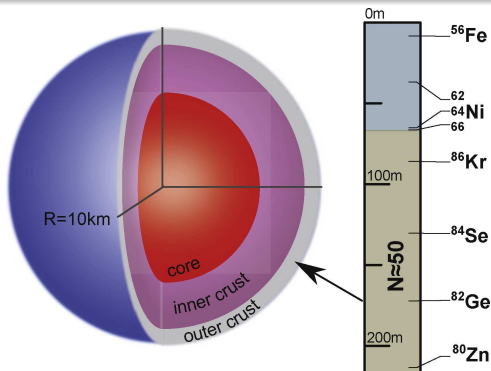
Pearson,Goriely,Chamel,Phys.Rev.C83,065810(2011)
Kreim, Hempel, Lunney, Schaffner-Bielich, Int.J.M.Spec.349-350,63(2013)
*Wolf et al.,PRL 110,041101(2013)*

Composition of the outer crust of a neutron star

Role of the symmetry energy

HFB-22-25 were fitted to different values of the symmetry energy coefficient at saturation, from $J = 29$ MeV (HFB-25) to $J = 32$ MeV (HFB-22).

HFB-22 (32)	HFB-24 (30)	HFB-25 (29)
^{79}Cu	-	-
^{82}Zn	-	-
^{78}Ni	^{78}Ni	^{78}Ni
^{80}Ni	^{80}Ni	-
-	-	^{126}Ru
^{124}Mo	^{124}Mo	^{124}Mo
^{122}Zr	^{122}Zr	^{122}Zr
^{121}Y	^{121}Y	^{121}Y
-	^{120}Sr	^{120}Sr
^{122}Sr	^{122}Sr	^{122}Sr
^{124}Sr	^{124}Sr	-
^{128}Sr	-	-
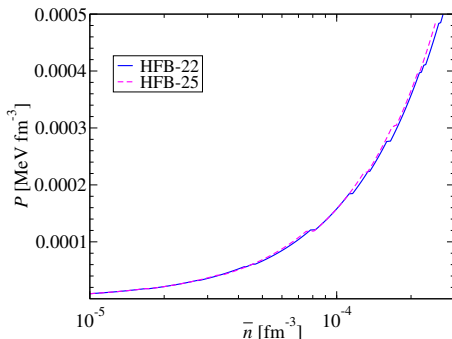
Composition of the outer crust of a neutron star

Role of the spin-orbit coupling

HFB-24: $v_{ij}^{\mathrm{so}} = \dfrac{i}{\hbar^2} W_0 (\boldsymbol{\sigma}_i + \boldsymbol{\sigma}_j) \cdot \boldsymbol{p}_{ij} \times \delta(\boldsymbol{r}_{ij}) \boldsymbol{p}_{ij}$

HFB-28: $v_{ij}^{\mathrm{so}} \rightarrow v_{ij}^{\mathrm{so}} + \dfrac{i}{\hbar^2} W_1 (\boldsymbol{\sigma}_i + \boldsymbol{\sigma}_j) \cdot \boldsymbol{p}_{ij} \times (n_{qi} + n_{qj})^{\nu} \delta(\boldsymbol{r}_{ij}) \boldsymbol{p}_{ij}$

HFB-29: $\mathcal{E}_{\mathrm{so}} = \dfrac{1}{2} \left[\boldsymbol{J} \cdot \nabla n + (1 + y_w) \displaystyle\sum_q \boldsymbol{J_q} \cdot \nabla n_q \right]$

HFB-28	HFB-29	HFB-24
^{79}Cu	^{79}Cu	-
^{78}Ni	^{78}Ni	^{78}Ni
^{128}Pd	-	-
^{80}Ni	-	^{80}Ni
^{126}Ru	^{126}Ru	-
^{124}Mo	^{124}Mo	^{124}Mo
^{122}Zr	^{122}Zr	^{122}Zr
-	^{121}Y	^{121}Y
^{120}Sr	^{120}Sr	^{120}Sr
^{122}Sr	^{122}Sr	^{122}Sr
^{124}Sr	^{124}Sr	^{124}Sr
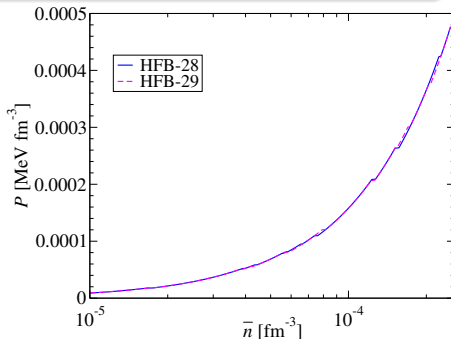
# Composition of the outer crust of a neutron star

Role of nuclear pairing

HFB-27* is based on an empirical pairing functional.
HFB-29 (HFB-30) was fitted to EBHF $^1S_0$ pairing gaps including medium polarization effects without (with) self-energy effects.

HFB-27*	HFB-29	HFB-30
-	^{79}Cu	-
^{78}Ni	^{78}Ni	^{78}Ni
-	-	^{80}Ni
^{126}Ru	^{126}Ru	^{126}Ru
^{124}Mo	^{124}Mo	^{124}Mo
^{122}Zr	^{122}Zr	^{122}Zr
-	^{121}Y	^{121}Y
^{120}Sr	^{120}Sr	^{120}Sr
^{122}Sr	^{122}Sr	^{122}Sr
^{124}Sr	^{124}Sr	^{124}Sr
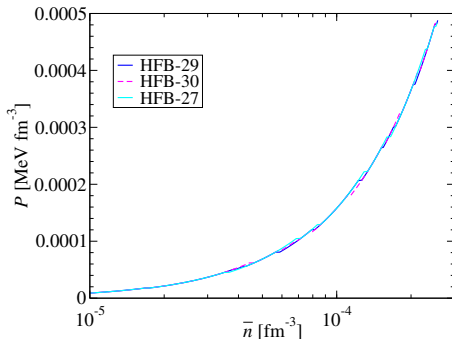
Catalyzed vs accreted crusts

The composition of accreted crusts can be substantially different: matter is not in full thermodynamical equilibrium !

Using the HFB-27* nuclear mass model and considering ^{56}Fe ashes:
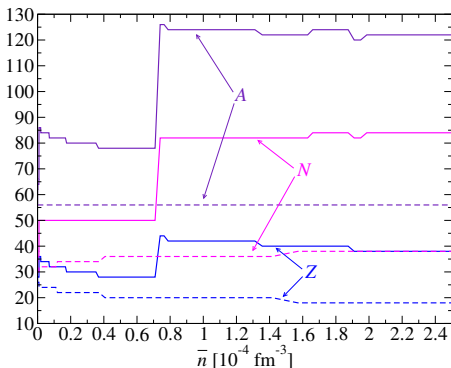
Chamel,Fantina,Zdunik,Haensel, Nuclear Theory 34, pp.126-131 (Heron Press, Sofia, 2015)

Stratification and equation of state

So far, we have assumed pure layers made of only one kind of nuclei
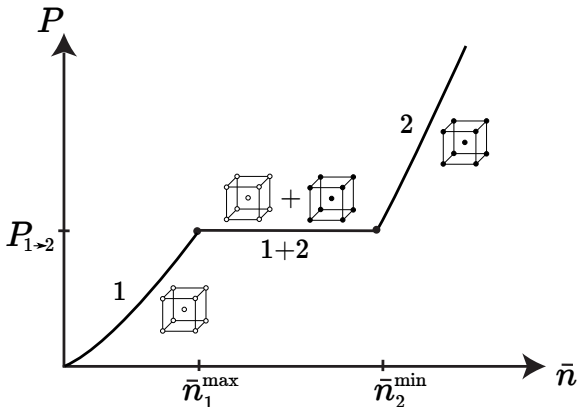
$$\frac{\bar{n}_2^{\min} - \bar{n}_1^{\max}}{\bar{n}_1^{\max}} \approx \frac{A_2}{Z_2} \frac{Z_1}{A_2} \left[1 + \frac{C_{\text{bcc}}\alpha}{(3\pi^2)^{1/3}} \left(Z_1^{2/3} - Z_2^{2/3} \right) \right] - 1$$

with $C_{\text{bcc}} = -1.444231$ and $\alpha = e^2/\hbar c$

Stratification and equation of state

So far, we have assumed pure layers made of only one kind of nuclei
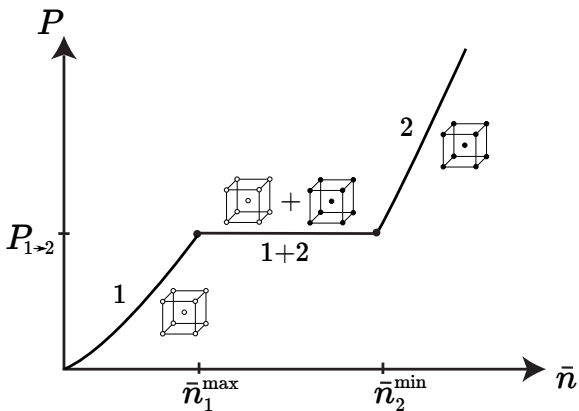
$$\frac{\bar{n}_2^{\min} - \bar{n}_1^{\max}}{\bar{n}_1^{\max}} > 0 \Rightarrow \frac{Z_2}{A_2} < \frac{Z_1}{A_1} : \text{ \textbf{the denser, the more neutron rich}}.$$

.

Stratification and equation of state

So far, we have assumed pure layers made of only one kind of nuclei
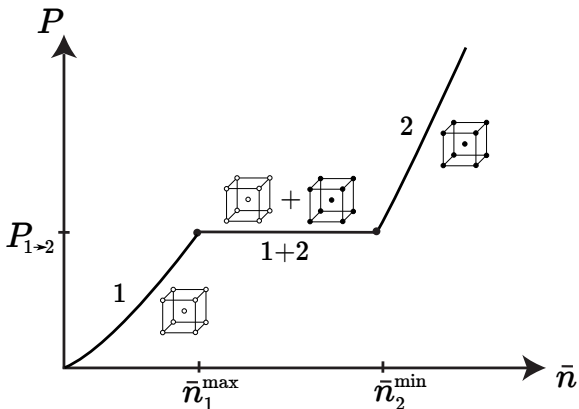
Mixed solid phases cannot exist in a neutron star crust because P has to increase strictly monotonically with $\bar{n}$.

Compounds in neutron-star crusts?

The structure could be determined using molecular dynamics simulations. However this would be extremely costly because the composition must be also optimized.

Multinary compounds made of nuclei with charges $\{Z_i\}$ could exist in the crust of a neutron star provided

- they are **stable against the separation into pure (bcc) phases**:

$$\mathcal{R}(\{Z_i/Z_j\}) \equiv \frac{C}{C_{\mathrm{bcc}}} f(\{Z_i\}) \frac{\bar{Z}}{\overline{Z^{5/3}}} > 1$$

  where $f(\{Z_i\})$ is the dimensionless lattice structure function of the compound and C the corresponding structure constant.
  Chamel & Fantina, Phys. Rev. C 94, 065802 (2016).

This condition is independent of the stellar environment and can thus be easily tested for any given compound structure and composition !

- they are **stable against weak and strong nuclear processes**.

Binary compounds in neutron-star crusts?

We have investigated the formation of various compounds:

fcc1   *fcc2*   *sc1*   *sc2*
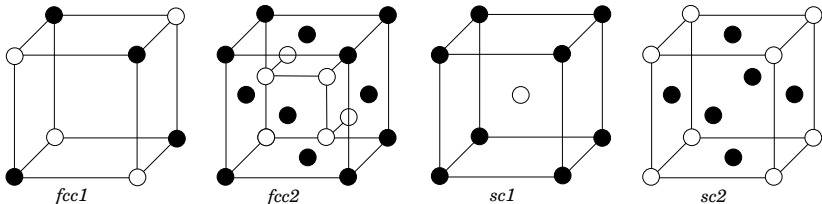
Terrestrial examples:

- fcc1: rocksalt (NaCl), oxydes, carbonitrides
- fcc2: fluorite (CaF_2)
- sc1: cesium chloride (CsCl), β-brass (CuZn)
- sc2: auricupride ($AuCu_3$)

Stellar compounds differ in two fundamental ways from their terrestrial counterparts: (i) they are made of nuclei; (ii) electrons form an essentially uniform relativistic Fermi gas.

Binary compounds in neutron-star crusts?

Oher cubic compounds with same structure as perovskites:
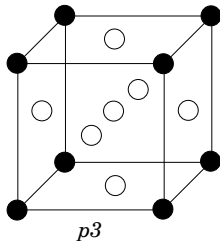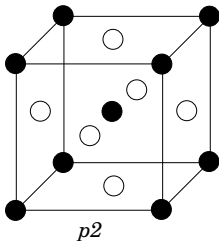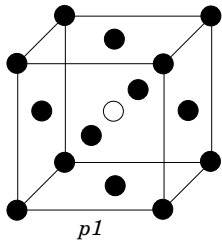
Non-cubic compounds (e.g. tungsten carbide):
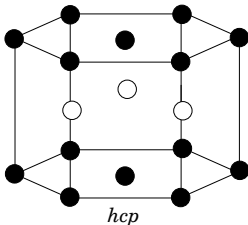
Binary compounds in neutron-star crusts?

Some compounds are unstable against phase separation for any charge ratio $q = Z_2/Z_1$ and can thus be ruled out:
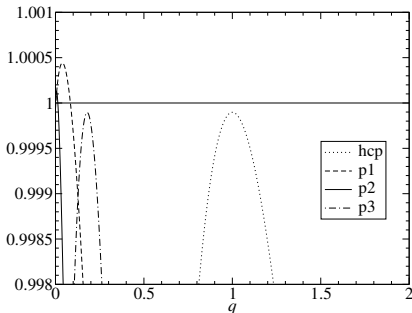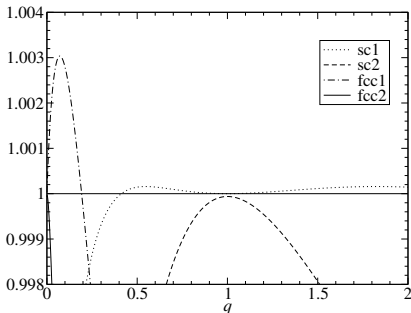

Chamel & Fantina, Phys. Rev. C 94, 065802 (2016).

The most likely compounds are those with CsCl structure.

Substitutional compounds in neutron-star crusts

Compounds with CsCl structure are present at interfaces if $Z_1 \neq Z_2$.
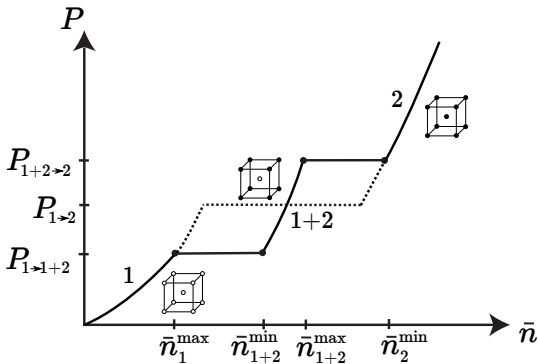
$$\frac{\bar{n}_{1+2}^{\text{max}} - \bar{n}_{1+2}^{\text{min}}}{\bar{n}_2^{\text{min}} - \bar{n}_1^{\text{max}}} \approx \frac{3 C_{\text{bcc}} \alpha}{(3\pi^2)^{1/3}} \frac{\tilde{f}(Z_1, Z_2) - \dfrac{\overline{Z^{5/3}}}{\bar{Z}}}{\left(1 - \dfrac{\bar{Z} A_1}{\bar{A} Z_1}\right)\left(1 - \dfrac{\bar{Z} A_2}{\bar{A} Z_2}\right)} \ll 1$$

Ternary compounds in neutron-star crusts?

We have also considered ternary compounds with cubic perovskite structure such as $BaTiO_3$:
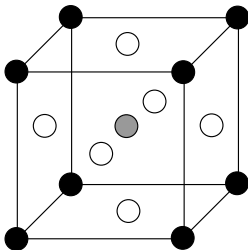
Such compounds do not exist in catalyzed crusts and but could be formed in accreting neutron stars.
Chamel, in preparation

Neutron-drip transition: general considerations

Nuclei are actually stable against neutron emission but are unstable against *electron captures* accompanied by neutron emission
$$^A_Z X + \Delta Z e^- \to ^{A-\Delta N}_{Z-\Delta Z} Y + \Delta N\, n + \Delta Z\, \nu_e$$
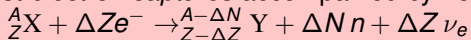
- **nonaccreting neutron stars**
  All kinds of reactions are allowed: the ground state is reached for $\Delta Z = Z$ and $\Delta N = A$

	outer crust	drip line	$\rho_{\rm drip}$ (g cm^{-3})	$P_{\rm drip}$ (dyn cm^{-2})
HFB-19	^{126}Sr (0.73)	^{121}Sr (-0.62)	4.40×10^{11}	7.91×10^{29}
HFB-20	^{126}Sr (0.48)	^{121}Sr (-0.71)	4.39×10^{11}	7.89×10^{29}
HFB-21	^{124}Sr (0.83)	^{121}Sr (-0.33)	4.30×10^{11}	7.84×10^{29}

- **accreting neutron stars**
  Multiple electron captures are very unlikely: $\Delta Z = 1$ ($\Delta N \geq 1$)

	$\rho_{\rm drip}$ (g cm^{-3})	$P_{\rm drip}$ (dyn cm^{-2})
HFB-21	$2.83 - 5.84 \times 10^{11}$	$4.79 - 12.3 \times 10^{29}$

$\rho_{\rm drip}$ and $P_{\rm drip}$ can be expressed by simple analytical formulas.
Chamel, Fantina, Zdunik, Haensel, Phys. Rev. C91,055803(2015).

Impact of a strong magnetic field on the crust?

In a strong magnetic field $\vec{B}$ (along let's say the z-axis), the **electron motion perpendicular to the field is quantized**:

Landau-Rabi levels
Rabi, Z.Phys.49, 507 (1928).

$e_\nu = \sqrt{c^2 p_z^2 + m_e^2 c^4 (1 + 2\nu B_\star)}$
where $\nu = 0, 1, ...$ and $\mathbf{B_\star} = \mathbf{B}/\mathbf{B_c}$
with $\mathbf{B_c} = \dfrac{\mathbf{m_e^2 c^3}}{\hbar \mathbf{e}} \simeq \mathbf{4.4 \times 10^{13}}$ G.

Maximum number of occupied Landau levels for HFB-21:

$B_\star$	1500	1000	500	100	50	10	1
ν_{max}	1	2	3	14	28	137	1365

Only $\nu = 0$ is filled for $\rho < 2.07 \times 10^6 \left(\dfrac{A}{Z}\right) B_\star^{3/2}$ g cm^{-3}.

Landau quantization can change the properties of the crust.

Equation of state of the outer crust of magnetars

Matter in a magnetar is much more **incompressible and less neutron-rich** than in a weakly magnetised neutron star.
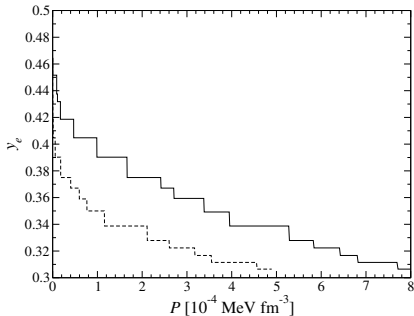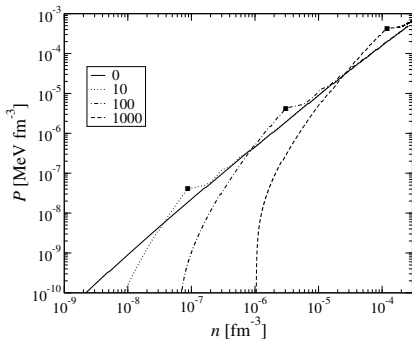
$$P \approx P_0 \left(\frac{n}{n_s} - 1 \right)^2$$

$$y_e \approx \frac{1}{2} \left(1 - \sqrt{\frac{\pi^2 \lambda_e^3 m_e c^2 P}{4 B_\star J^2}} \right)$$

Chamel et al.,Phys.Rev.C86, 055804(2012).

Composition of the outer crust of a magnetar

The magnetic field changes the composition:

Equilibrium nuclides for HFB-24 and $B_\star \equiv B/(4.4 \times 10^{13}$ G):

Nuclide	$B_\star$
^{58}Fe(-)	9
^{66}Ni(-)	67
^{88}Sr(+)	859
^{126}Ru(+)	1031
^{80}Ni(-)	1075
^{128}Pd(+)	1445
^{78}Ni(-)	1610
^{79}Cu(-)	1617
^{64}Ni(-)	1668
^{130}Cd(+)	1697
^{132}Sn(+)	1989
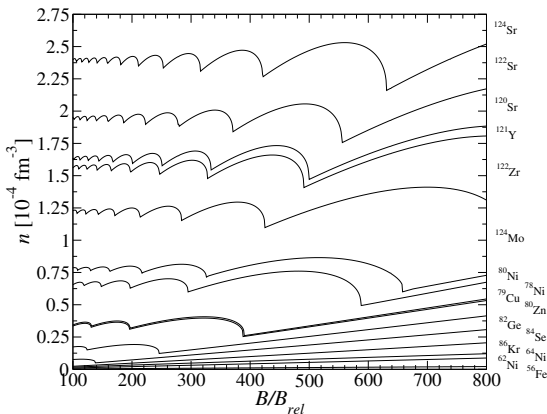
Chamel et al., to appear in QSCP series, Springer (2017).

Neutron-drip transition in magnetars


These oscillations are almost universal:

$$\frac{n_{\rm drip}^{\min}}{n_{\rm drip}(B_\star = 0)} \approx \frac{3}{4}$$

$$\frac{n_{\rm drip}^{\max}}{n_{\rm drip}(B_\star = 0)} \approx \frac{35 + 13\sqrt{13}}{72}$$

In the strongly quantizing regime,

$$n_{\rm drip} \approx \frac{A}{Z} \frac{\mu_e^{\rm drip}}{m_e c^2} \frac{B_\star}{2\pi^2 \lambda_e^3} \left[1 - \frac{4}{3} C\alpha Z^{2/3} \left(\frac{B_\star}{2\pi^2} \right)^{1/3} \left(\frac{m_e c^2}{\mu_e^{\rm drip}} \right)^{2/3} \right]$$

Chamel et al.,Phys.Rev.C91, 065801(2015).
Chamel et al.,J.Phys.:Conf.Ser.724, 012034 (2016).

Neutron-drip transition in magnetars
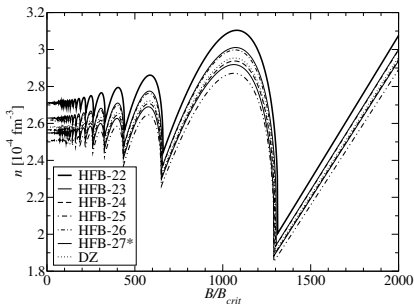
These oscillations are almost universal:

$$\frac{n_{\rm drip}^{\rm min}}{n_{\rm drip}(B_\star = 0)} \approx \frac{3}{4}$$

$$\frac{n_{\rm drip}^{\rm max}}{n_{\rm drip}(B_\star = 0)} \approx \frac{35 + 13\sqrt{13}}{72}$$

In the strongly quantizing regime,

$$n_{\rm drip} \approx \frac{A}{Z}\frac{\mu_e^{\rm drip}}{m_e c^2}\frac{B_\star}{2\pi^2\lambda_e^3}\left[1 - \frac{4}{3}C\alpha Z^{2/3}\left(\frac{B_\star}{2\pi^2}\right)^{1/3}\left(\frac{m_e c^2}{\mu_e^{\rm drip}}\right)^{2/3}\right]$$

Chamel et al.,Phys.Rev.C91, 065801(2015).
Chamel et al.,J.Phys.:Conf.Ser.724, 012034 (2016).

Neutron-drip transition: role of the symmetry energy

The lack of knowledge of the symmetry energy translates into uncertainties in the neutron-drip density:
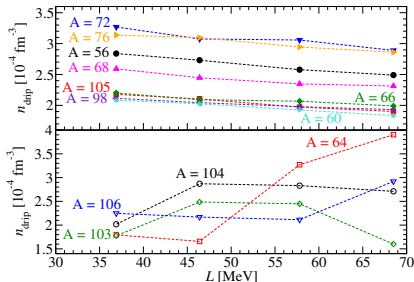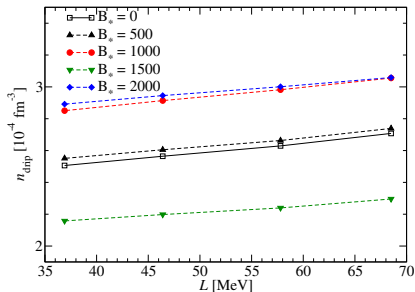
In accreted crusts, the neutron-drip transition may be more sensitive to nuclear-structure effects than the symmetry energy.

Fantina et al.,Phys.Rev.C93,015801(2016).

Description of neutron star crust beyond neutron drip

We use the **Extended Thomas-Fermi+Strutinsky Integral (ETFSI)** approach with the *same* functional as in the outer crust:

- **semiclassical expansion in powers of** $\hbar^2$: the energy becomes a functional of $n_q(\boldsymbol{r})$ and their gradients only.
- **proton shell effects** are added perturbatively (neutron shell effects are much smaller and therefore neglected).

In order to further speed-up the calculations, clusters are supposed to be spherical (no pastas) and $n_q(\boldsymbol{r})$ are parametrized.

Pearson,Chamel,Pastore,Goriely,Phys.Rev.C91, 018801 (2015).
Pearson,Chamel,Goriely,Ducoin,Phys.Rev.C85,065803(2012).
Onsi,Dutta,Chatri,Goriely,Chamel,Pearson, Phys.Rev.C77,065805 (2008).

Advantages of the ETFSI method:

- very fast approximation to the full HFB equations
- avoids the difficulties related to boundary conditions
  Chamel et al.,Phys.Rev.C75(2007),055806.

Structure of nonaccreting neutron star crusts

With increasing density, the clusters keep essentially the same size but become more and more dilute.

The crust-core transition predicted by the ETFSI method agrees very well with the instability analysis of homogeneous nuclear matter.

	$\bar{n}_{cc}$ (fm^{-3})	P_{cc} (MeV fm^{-3})
BSk27*	0.0919	0.439
BSk25	0.0856	0.211
BSk24	0.0808	0.268
BSk22	0.0716	0.291
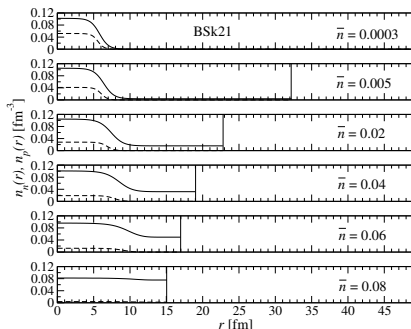
*Chamel et al., Acta Phys. Pol.46,349(2015).*
Pearson,Chamel,Goriely,Ducoin,Phys.Rev.C85,065803(2012).

The crust-core transition is found to be very smooth.

Role of proton shell effects on the composition of the inner crust of a neutron star

- The ordinary nuclear shell structure seems to be preserved apart from $Z = 40$ (quenched spin-orbit?).
- The energy differences between different configurations become very small as the density increases!

ETF: dashed lines - ETFSI: solid lines
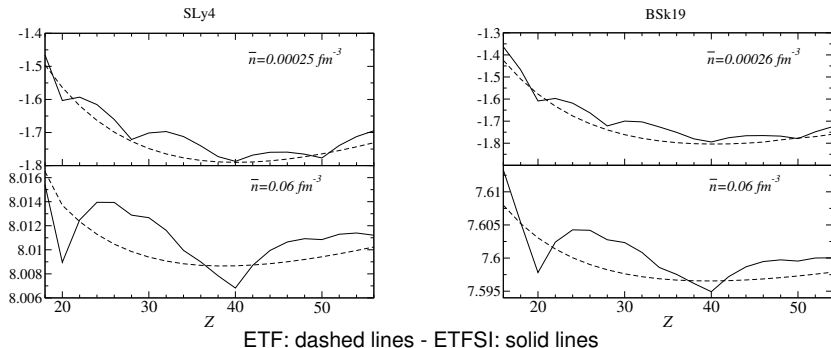
Role of proton pairing on the composition of the inner crust of a neutron star

Proton shell effects are washed out due to pairing.
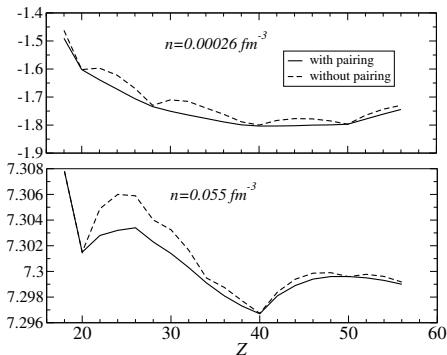
Example with BSk21.

At low densities, $Z = 42$ is energetically favored over $Z = 40$, but by less than 5×10^{-4} MeV per nucleon.

A large range of values of Z could thus be present in a real neutron-star crust.

Pearson,Chamel,Pastore,Goriely,Phys.Rev.C91, 018801 (2015).

Due to proton pairing, the inner crust of a neutron star is expected to contain many impurities.

Unified equations of state of neutron stars

The same functionals used in the crust can be also used in the core (n, p, e^-, μ^-) thus providing a **unified and thermodynamically consistent description of neutron stars**.

- **Tables** of the full equations of state for HFB-19, HFB-20, and HFB-21:

  http://vizier.cfa.harvard.edu/viz-bin/VizieR?-source=J/A+A/559/A128
 *Fantina, Chamel, Pearson, Goriely, A&A 559, A128 (2013)*

- **Analytical representations** of the full equations of state (fortran subroutines):

  http://www.ioffe.ru/astro/NSG/BSk/
  Potekhin, Fantina, Chamel, Pearson, Goriely, A&A 560, A48 (2013)

Equations of state for our latest functionals will appear soon.

Nuclear uncertainties in the mass-radius

Mass-radius relation of nonrotating and nonaccreting neutron stars:
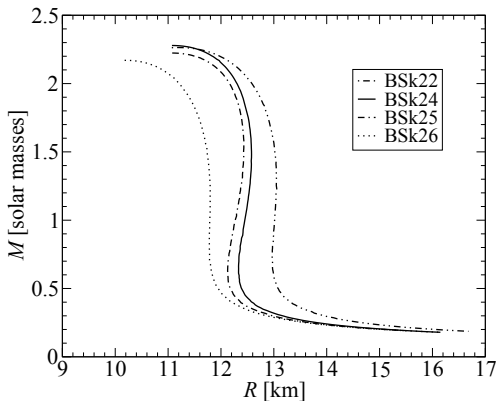
The radius of a $1.4 M_\odot$ neutron star is predicted to lie between 11.8 and 13 km.

Delsate et al., Phys. Rev. D 94, 023008 (2016)

Conclusions

- We have developed **accurately calibrated nuclear energy density functionals** fitted to essentially all nuclear mass data as well as to microscopic calculations.
- These functionals provide a **unified and consistent description of neutron-star crusts**.
- **The equation of state of the outer crust is fairly well known**, but its composition depends on the nuclear structure of very exotic nuclei (e.g. spin-orbit coupling, pairing).
- **The constitution of the inner crust is much more uncertain** due to the tiny energy differences between different configurations (nuclear pastas?)
- **Magnetars may have different crusts**.

Systematic studies of crustal properties for both nonaccreted and accreted neutron stars are under way.